VOL. 9, NO. 10, OCTOBER 2014 ISSN 1819-6608
ARPN Journal of Engineering and Applied Sciences

www.arpnjournals.com

PRESSURE AND PRESSURE DERIVATIVE ANALYSIS FOR HYDRAULICALLY-FRACTURED SHALE FORMATIONS USING THE CONCEPT OF INDUCED PERMEABILITY FIELD

Karla María Bernal[1], Freddy Humberto Escobar[1] and Alfredo Ghisays-Ruiz[2]
[1]Universidad Surcolombiana/CENIGAA, Avenida Pastrana - Cra 1, Neiva, Huila, Colombia
[2]Universidad del Atlantico, Fac. de Ciencias Básicas. antigua vía Puerto Colombia, Barranquilla, Atlantico, Colombia
E-Mail: fescobar@usco.edu.co

ABSTRACT

An appropriate characterization of such unconventional resources as shale formations requires the availability of practical and accurate tools. Wells drilled in shale formations have to be hydraulically fractured for commercial production since the permeability is very low to ultralow reaching values in the order of nanodarcies. If these formations are tested by keeping constant the flow rate, then, there is a need of providing a pressure-transient interpretation technique which in this research follows the *TDS* philosophy. Contrary to transient-rate analysis where a third flow regime is observed during the transition period between linear and pseudosteady state which allows for the model identification, in transient-pressure analysis that period does not exist so identification of the permeability model cannot be obtained. Therefore, the developed equations for permeability, half-fracture length, skin factor and reservoir length are used without considering the model. The equations were successfully tested with synthetic examples.

Keywords: shale formations, superposition, flow regimes, transient-rate analysis, average reservoir pressure.

1. INTRODUCTION

The exploiting of hydrocarbons from shale formations is becoming more important every day. Then, there is a need of providing practical and accurate techniques for the characterization of pressure tests in such formations. In order to make them feasible to exploit, hydraulic fracturing must be performed. This causes the presence not only of microfractures with an increase reservoir permeability but also linear flow regime and late pseudosteady-state period which are required to be carefully analyze.

Among the researches aimed to study the behavior of fractured shales, we can name the works of Palmer, Moschovidis, and Cameron (2007), and Ge and Ghassemi (2011). The models presented by Wattenbarger *et al*. (1998) and El-Banbi and Wattenbarger (1998) assume uniform permeability in the surroundings of the fracture system which may not be the proper case. Recently, Fuentes-Cruz, Gildin and Valko (2014) presented a mathematical model considering that the average effect of the failure of weak planes leads to a non-uniform permeability distribution depending on the distance to the hydraulic fracture which becomes the basis of this work. They considered three permeability variation models: uniform, linear and exponential. Their reservoir characterization was conducted by using rate-decline analysis which was later extended to transient-rate and reciprocal rate derivative analysis by Escobar, Montenegro and Bernal (2014) by following the *TDS* philosophy, Tiab (1993).

No permeability variation effect was found on the pressure and pressure derivative curves since the authors believe than the transient pressure travel faster than the transient rate disturbance. Then, by using pressure-transient analysis no model can be differentiated and, then, same equations were developed for the three models which were successfully tested with synthetic examples.

2. MATHEMATICAL FORMULATION

2.1. Mathematical model

This study is based upon the mathematical model introduced by Cruz-Fuentes *et al*. (2014) as given below which dimensionless Laplacian pressure solution, $\bar{P}_D$, for the exponential, linear and uniform permeability fields are respectively given as:

$$\bar{P}_D = \frac{\delta\pi}{u\sqrt{u}}\left[\frac{I_1\left(\frac{2y_D^*\sqrt{u}}{\ln(\xi)}\right)K_0\left(\frac{2y_D^*}{\ln(\xi)}\sqrt{\frac{u}{k_D^*}}\right)+I_0\left(\frac{2y_D^*}{\ln(\xi)}\sqrt{\frac{u}{k_D^*}}\right)K_1\left(\frac{2y_D^*\sqrt{u}}{\ln(\xi)}\right)}{I_0\left(\frac{2y_D^*\sqrt{u}}{\ln(\xi)}\right)K_0\left(\frac{2y_D^*}{\ln(\xi)}\sqrt{\frac{u}{k_D^*}}\right)-I_0\left(\frac{2y_D^*}{\ln(\xi)}\sqrt{\frac{u}{k_D^*}}\right)K_0\left(\frac{2y_D^*\sqrt{u}}{\ln(\xi)}\right)}\right] \quad (1)$$

(If $k_D^*<1$, δ=-1 and ξ=1/ k_D^*; if $k_D^*>1$, δ=1 and ξ= k_D^*)

$$\bar{P}_D = \frac{\delta\pi}{u\sqrt{u}}\left[\frac{I_1\left(\frac{2y_D^*\sqrt{k_D^*u}}{\left|K^*_D-1\right|}\right)K_0\left(\frac{2y_D^*\sqrt{u}}{\left|K^*_D-1\right|}\right)+I_0\left(\frac{2y_D^*\sqrt{u}}{\left|K^*_D-1\right|}\right)K_1\left(\frac{2y_D^*\sqrt{k_D^*u}}{\left|K^*_D-1\right|}\right)}{I_1\left(\frac{2y_D^*\sqrt{k_D^*u}}{\left|k_D^*-1\right|}\right)K_1\left(\frac{2y_D^*\sqrt{u}}{\left|k_D^*-1\right|}\right)-I_1\left(\frac{2y_D^*\sqrt{u}}{\left|k_D^*-1\right|}\right)K_1\left(\frac{2y_D^*\sqrt{k_D^*u}}{\left|k_D^*-1\right|}\right)}\right] \quad (2)$$

(If $k_D^*<1$, δ=-1; $k_D^*>1$, δ=1)

$$\bar{P}_D = \frac{\pi}{u\sqrt{u}}\coth\left(y_D^*\sqrt{u}\right) \quad (3)$$

Where I_v and K_v are the modified Bessel functions of first and second kind, respectively (v=0, 1). The dimensionless time for oil and gas wells in field units is,

$$t_D = \frac{0.0002637k^0t}{\phi(\mu c_t)_i x_e^2} \quad (4)$$

The dimensional length stimulated reservoir volume.

$$y_D = \frac{y}{x_e} \tag{5}$$

The dimensionless permeability quantities for exponential and linear cases, respectively, are,

$$k_D(y_D) = \frac{k(y)}{k^0} = k_D^{*(y_D/y_D^*)} = e^{(\ln k_D^*)^{*(y_D/y_D^*)}} \tag{6}$$

$$k_D(y_D) = \frac{k(y)}{k^0} = 1 + (k_D^* - 1)\left(y_D / y_D^*\right) \tag{7}$$

The dimensionless minimum permeability is given also as,

$$k_D^* = \frac{k^*}{k^0} \tag{8}$$

The definitions of dimensionless gas pseudopressure and the pseudopressure derivative, respectively in the solution for constant production rate, are:

$$P_D = \frac{n_{HF} k^0 h\left[m(P_i) - m(P_{wf})\right]}{1424\ T\ q_w} \tag{9}$$

$$t_D * m(P_D)' = \frac{n_{HF} k^\circ h}{1424\ q_w T}\left[t * [\Delta m(P)'\right] \tag{10}$$

The dimensionless oil pressure and the pressure derivative, respectively, are:

$$P_D = \frac{n_{HF} k^0 h\left(P_i - P_{wf}\right)}{141.2\ B_o q\ \mu_o} \tag{11}$$

$$\left[t_D * (P_D)'\right] = \frac{n_{HF} k^\circ h}{141.2\ q\ B_o \mu_o}\left[t * \Delta P'\right] \tag{12}$$

Using the concept of stimulated reservoir volume, the half-length of the hydraulic fracture ($2x_f$) is equal to the lateral extent of the volume that is stimulated, Fuentes-Cruz *et al*. (2014):

$$2x_f = x_e \tag{13}$$

2.2. *TDS* formulation for linear flow regime

The early-time linear flow regime is seen in the three above mentioned models: uniform, linear and exponential. It is characterized by a typical 0.5-slope line on the pressure derivative curve. Notice also that this flow regime shows up at about the same time period for y_D values as shown in Figures 1 through 3. Therefore, its behavior does not depend upon neither the variation of the dimensionless reservoir length nor the minimum permeability value.

The early time portion of the log-log plot of dimensionless pseudopressure versus dimensionless time with constant k_D and variable y_D is used for the determination of the linear flow regime governing equation. The equation works independently of the permeability model since represents the maximum induced permeability in the stimulated reservoir volume, SRV:

$$t_D * m(P_D)' = \frac{5.74}{\pi}\sqrt{t_D} \tag{14}$$

Once the dimensionless quantities given by Equations (4) and (10) are replaced into Equation (14), it yields;

$$\frac{n_{HF} k^\circ h}{1424\ q\ T}\left[t * [\Delta m(P)'\right] = \frac{5.74}{\pi}\left(\frac{0.0002637 k^\circ t}{\phi(\mu c_t)_i x_e^2}\right)^{0.5} \tag{15}$$

Since linear flow is independent of the minimum permeability -at the end of the main plane of fracture- Equation (15) allows obtaining an expression for the determination of the maximum induced permeability, k^0, by reading the values of pseudopressure derivative at any arbitrary time during linear flow regime, so that:

$$k^\circ = \frac{1785.065\ t_L}{\phi(\mu c_t)_i x_e^2}\left(\frac{q\ T}{n_{HF} h\left[t * [\Delta m(P)'\right]_L}\right)^2 \tag{16}$$

Notice that the reservoir length, x_e, can be solved from Equation (16),

$$x_e = \frac{42.25\ q_w T}{n_{HF} h\left[t * [\Delta m(P)'\right]_L}\sqrt{\frac{t_L}{\phi(\mu c_t)_i k^\circ}} \tag{17}$$

The dimensionless pressure expression is found by integration of Equation (14), then,

$$m(P)_D = s_L - \frac{2.87}{\pi}\left(t_D\right)_L^{0.5} \tag{18}$$

An expression for the geometrical skin factor, s_L, is obtained from the division of Equation (18) by Equation (14) and solving for s_L,

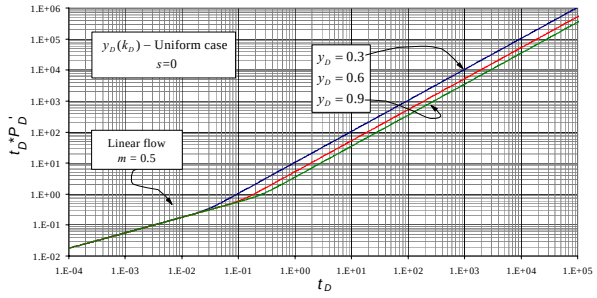

Figure-1. Effect of the dimensionless reservoir length (y_D*) on the flow behavior for the uniform case, (k_D*=0.15).

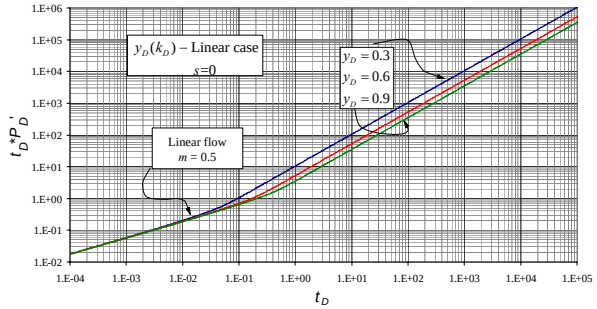

Figure-2. Effect of the dimensionless reservoir length (y_D*) on the flow behavior for the linear case, (k_D*=0.1).

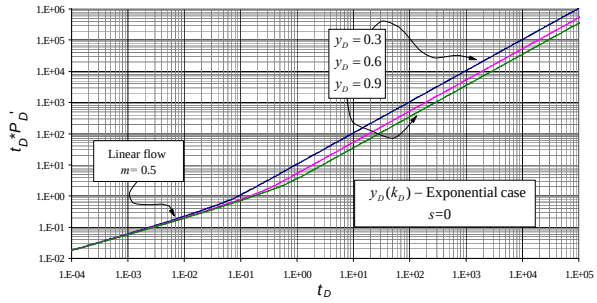

Figure-3. Effect of the dimensionless reservoir length (y_D*) on the flow behavior for the exponential case, (k_D*=0.1).

$$s_L = \frac{5.74}{\pi}(t_D^{0.5})_L \left[\frac{[m(P)_D]_L}{[t_D * m(P)'_D]_L} + \frac{1}{2}\right] \quad (19)$$

After plugging equations (9) and (10) into Equation (19), it yields in dimensional form,

$$s_L = 0.030\left(\frac{kt_L}{\phi(\mu c_t)_i x_e^2}\right)^{0.5}\left[\frac{\Delta m(P)_L}{[t * \Delta m(P)']_L} + \frac{1}{2}\right] \quad (20)$$

2.3. *TDS* Formulation for pseudosteady-state regime

The determination of the governing equation for the late pseudosteady period requires a log-log plot of t_D*P_D' or t_D*$m(P)_D$' versus t_{DA} using a dimensionless constant permeability (k_D = constant) and different dimensionless length values (y_D= 0.1, 0.6 and 0.9), for each one of the induced permeability models as shown in Figures-3 through 5. In each model, a uniform behavior was found by dividing the dimensionless time by the dimensionless length of the stimulated reservoir volume for each case, respectively.

$$t_{DA} = \frac{t_D}{y_D^2} \quad (21)$$

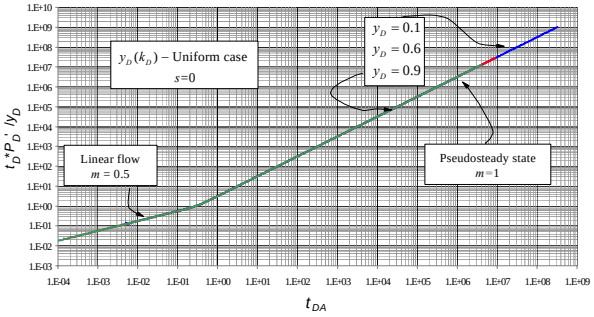

Figure-4. Effect of the variation of the dimensionless length on the pseudosteady state regime for the uniform model with k_D constant.

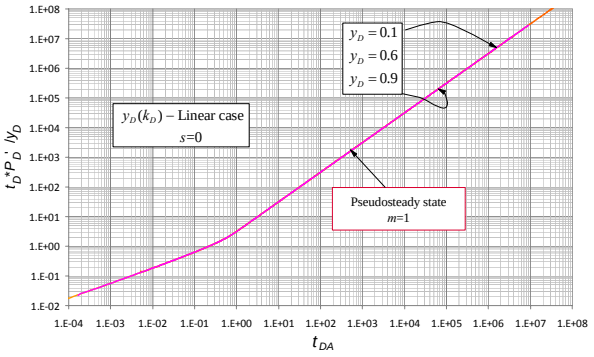

Figure-5. Effect of the variation of the dimensionless length on the pseudosteady state regime for the linear model with k_D constant.

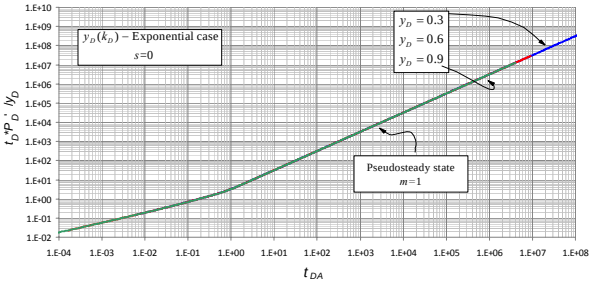

Figure-6. Effect of the variation of the dimensionless length on the pseudosteady state regime for the exponential model with k_D constant.

The late pseudosteady-state regime is used for the calculation of the well drainage area whether or not the permeability value is known.

As seen in Figures 1 through 3, the late time pseudosteady-state regime is shown as a unit-slope straight line. It is important to remark that in transient-pressure analysis this behavior is independent of the permeability model, see Figure-6, while in transient-rate analysis the behavior of the late pseudosteady-state regime is particular for each model as indicated by Escobar *et al*. (2014), see Figure-7. This leads to point out the existence of a transition period between the linear flow regime and the pseudosteady-state period for the exponential and linear cases which indicates a permeability variation from the main fracture plane to the remaining SRV.

Besides, contrary to the case of transient-rate analysis as determined by Escobar *et al*. (2014), in pressure-transient analysis is observed that the transition period between linear and pseudosteady state is so small that a relationship cannot be established. In the work presented by Escobar *et al*. (2014) this transition was so remarked that it was represented by a possible flow regime which they called "multilinear".

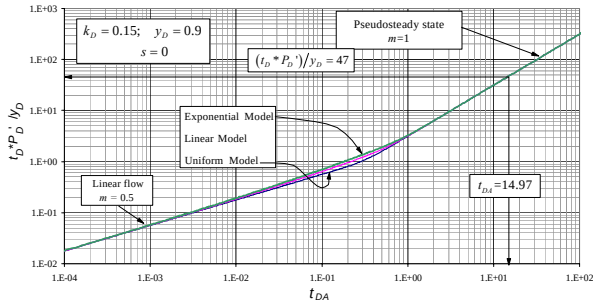

Figure-7. Dimensionless pressure derivative behavior versus time for the three dealt models.

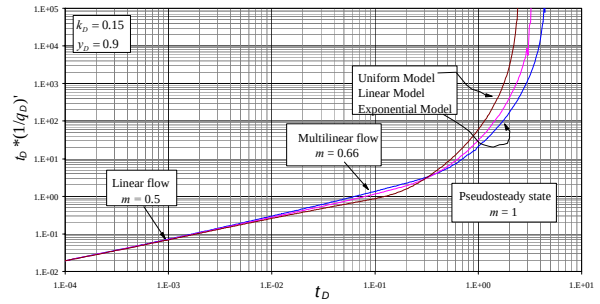

Figure-8. Dimensionless reciprocal rate derivative behavior versus time for the three dealt models as described by Escobar *et al*. (2014).

Then, it is possible to write a general dimensionless pressure or pseudopressure derivative expression for the pseudosteady state period, for the three models is given as follows,

$$\frac{\left[t_D * P_D'\right]_{PSS}}{y_D} = \pi\left(\frac{t_D}{y_D^2}\right)_{PSS} \tag{22}$$

After the dimensionless terms given by Equations (4), (5) and (10) are replaced in Equation (22), an expression for the determination of the lateral reservoir length, x_e, is obtained,

$$x_e = \frac{\pi(0.0002637)(1424)T\,q_w}{n_{hf}\phi h(\mu c_t)_i\, y}\frac{t_{PSS}}{\left[t * \Delta m(P)'\right]_{PSS}} \tag{23}$$

Opposite to the methodology proposed by Escobar *et al*. (2014) at late time where is necessary to find a parameter called α -which depends upon the permeability model- in transient-pressure analysis there is no distinction of the permeability variation from the main fracture plane, then, a unique expression for the three models is obtained.

2.5. Interception point

Permeability can be verified from an expression obtained by using the intersection point formed by the radial flow regime and the late-time pseudosteady-state period. By manipulation of Equations (14) and (22), it yields;

$$\left(\frac{0.0002637k^{\circ}t_{LPSSi}}{\phi(\mu c_t)_i}\right)^{0.5} = 0.5816y \tag{24}$$

Equation (24) allows solving for the maximum induced permeability,

$$k^{\circ} = \left[\frac{1282.254y^2\left[\phi(\mu c_t)_i\right]}{t_{LPSS_i}}\right] \tag{25}$$

The work presented by Escobar *et al*. (2014) also permitted to use the point of intercept between the late pseudosteady state and the so-called "multilinear flow" which represents the permeability variations at the SRV's extreme boundaries. This flow regime leads to the estimation of the minimum induced permeability. This flow regime is unobserved when using pressure-transient analysis, and then, it is not possible the estimation of the minimum induced permeability.

Equations for oil flow are presented in appendix-A.

Table-1. Relevant information for the uniform model.

Parameter	Value	Parameter	Value
h (ft)	700	μ_g (cp)	0.011
ϕ (%)	6.32	x_e (ft)	1350
T (°R)	590.8	c_t (psi^{-1})	2.53x10^{-5}
B_{gi} (rb/Mscf)	0.825	y (ft)	502.2
k (md)	0.0106	# stages	2
q (Mscf/day)	239223.2	s	0

4. EXAMPLES

Three synthetic examples are worked for the applicability of the above developed equations for each model. Table-1 provides relevant information of the reservoir, well and fluid properties used in each one of the permeability models.

4.1. Example-1. Uniform model

For the case under consideration, the pseudopressure drop and its derivative against time are reported in Figure-8 with the purpose of determining the permeability, half-fracture length and reservoir length.

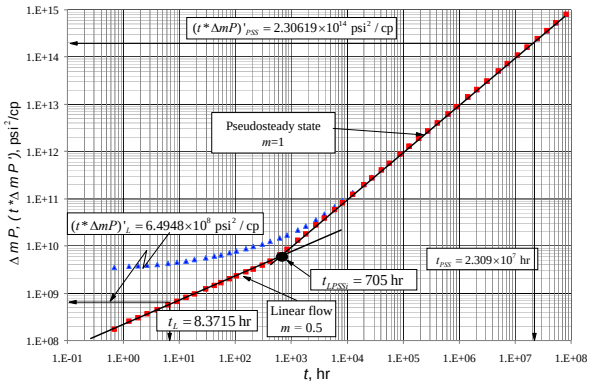

Figure-9. Log-log plot of the pseudopressure and pseudopressure derivative vs. time for the uniform synthetic example.

Solution. As expected for this example, only linear flow regime and pseudosteady state period are developed and observed. The below parameters were read from Figure-8.

t_L = 8.37153 hr
$\Delta m(P)_L$ = 4.49x10^9 psi^2/cp
$[t*\Delta m(P)']_L$ = 6.4948x10^8 psi^2/cp
t_{PSS} = 2.30878x10^7 hr
$\Delta m(P)_{PSS}$ = 2.30627x10^{14} psi^2/cp
$[t*\Delta m(P)']_{PSS}$ = 2.30619x10^{14} psi^2/cp
t_{LPSSi} = 498 hr

Equation (16) applied on the linear flow regime is ideal for calculating the maximum induced permeability which resulted to be 0.011263 md. Then, Equation (17) allows calculating a value of x_e equal to 1366.05 ft which used in Equation (13) gives a value of half-fracture length of 683.025 ft. An initial skin factor of 0.3700 is found with Equation (20).

The pseudosteady-state regime is used along with Equation (23) to provide a value of x_e of 1349.9175 ft and the point of intersection used in Equation (39) gives a maximum permeability value of 0.01145 md.

Needless to say that there is no permeability variation in the uniform model; therefore, it does not exist any analyzable transition period between the linear flow regime and the pseudosteady state.

4.2. Example-2. Linear model

It is required to find permeability, reservoir length and half-fracture length from the data reported in Figure-9 and the information given in Table-2.

Table-2. Relevant information for the linear model.

Parameter	Value	Parameter	Value
h (ft)	853	c_t (psi^{-1})	2.53x10^{-5}
ϕ (%)	7.56	y (ft)	777
T (°R)	852	# stages	3
B_{gi} (rb/Mscf)	0.825	x_e (ft)	1110
μ_g (cp)	0.01	k (md)	0.005
q (Mscf/day)	239223.2	s	0

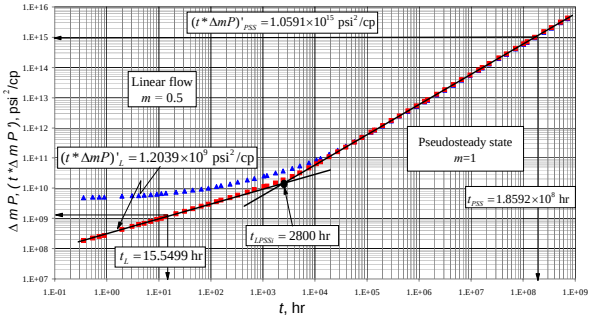

Figure-10. Log-log plot of the pseudopressure and pseudopressure derivative vs. time for the linear synthetic example.

Solution. For the application of the governing equations of each flow in this example, the following data are read from Figure-9,

t_L = 15.5499 hr
$\Delta m(P)_L$ = 6.9264x10^9 psi^2/cp
$[t*\Delta m(P)']_L$ = 1.2039x10^9 psi^2/cp
t_{PSS} = 1.8592x10^8 hr
$\Delta m(P)_{PSS}$ = 1.05914x10^{15} psi^2/cp
$[t*\Delta m(P)']_{PSS}$ = 1.05911x10^{15} psi^2/cp
t_{LPSSi} = 2800 hr

Application of Equation (16) on the linear flow regime leads to estimate a maximum induced permeability value of 0.005155 md. Then, Equation (17) is used to calculate a value of x_e of 1127.12 ft which used in Equation (13) gives a value of half-fracture length of 563.56 ft. An initial skin factor of 0.472 is found with Equation (20).

The pseudosteady state regime is used along with Equation (23) to find a value of x_e equal to 1109.829 ft and the intersection point, t_{LPSSi}, is used in Equation (39) to

estimate the maximum permeability value which resulted to be 0.00529 md.

4.3. Example-3. Exponential model

Figure-10 presents synthetic pseudopressure and pseudopressure derivative versus time data for an exponential model simulated using information from Table-3. It is required to properly characterize the reservoir by transient-pseudopressure analysis.

Table-3. Relevant information for exponential model.

Parameter	Value	Parameter	Value
h (ft)	1003	c_t (psi^{-1})	2.53x10^{-5}
ϕ (%)	8.20	y (ft)	711.5
T (°R)	912	# stages	4
B_{gi} (rb/Mscf)	0.825	x_e (ft)	1423
μ_g (cp)	0.01	k (md)	0.3
q (Mscf/dia)	3256310	s	0

Solution. The following information was read from Figure-12.

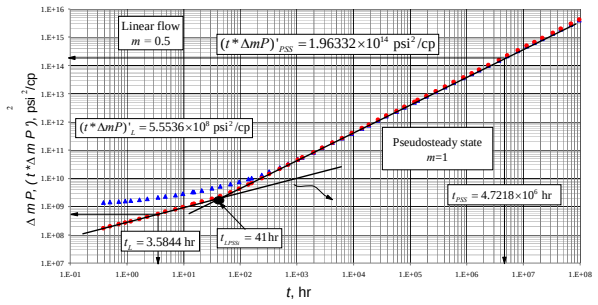

Figure-11. Log-log plot of the reciprocal rate and the reciprocal rate derivative vs. time for the exponential synthetic example.

t_L = 3.5844 hr
$\Delta m(P)_L$ = 2.1215x10^9 psi^2/cp
$[t^*\Delta m(P)']_L$ = 5.5536x10^8 psi^2/cp
t_{PSS} = 4.7218x10^6 hr
$\Delta m(P)_{PSS}$ = 1.96336x10^{14} psi^2/cp
$[t^*\Delta m(P)']_{PSS}$ = 1.96332x10^{14} psi^2/cp
t_{LPSSi} = 41 hr

Again, the maximum induced permeability is found with Equation (16). This resulted to be 0.2706 md. Afterwards, Equation (17) allows estimating a x_e value of 1351.419 ft which used in Equation (13) to provide a value of half-fracture length of 675.71 ft. An initial skin factor of 1.3145 is found with Equation (20).

The pseudosteady state regime is used along with Equation (23) provides a value x_e of 1422.781 ft and the point of intersection used in Equation (39) provides a maximum permeability value of 0.328 md.

5. CONCLUSIONS

a) New expressions for the interpretation of pressure-transient tests in such very low permeability formations as shales is presented using characteristic points on the pressure (pseudopressure) and pressure (pseudopressure) derivative versus time log-log plot. The equations were successfully tested with simulated examples so half-fracture length, permeability and skin factor values were found with a very good agreement compared to the input data.

b) Contrary to rate-transient analysis for systems under the same induce permeability model, there is no transition period observed in the pressure derivative between the linear flow regime and pseudosteady-state period. This makes impossible to distinguish among the three permeability model. This may be due to the fact that the transient pressure wave travels faster than the rate transient disturbance.

c) The pressure and pressure derivative behavior do not discriminate the permeability variation in the main fracture plane, according to the concept of the SRV as pointe out by Fuentes-Cruz *et al*. (2014), in each one of the three permeability models. This situation leads to the development of general expressions for finding permeability, skin factor, half-fracture length and the lateral reservoir boundary without considering the reservoir model. This situation is not the same for the case of transient-rate analysis as presented by Escobar *et al*. (2014).

Nomenclature

B_g	Volumetric factor, rb/Mscf
c_t	System total compressibility, 1/psi
k^0	Maximum Permeability induced, md
k^*	Minimum Permeability induced, md
$m(P)$	Pseudopressure, psi^2/cp
n_f	Number of main fracture planes
P	Pressure, psi
$\bar{P}$	Laplace-space pressure
P_{wf}	Bottomhole flowing pressure, psi
q	Flow rate (STB/D for oil, Mscf/D) for gas)
$1/q$	Reciprocal flow rate, D/Mscf
$t^*(1/q)'$	Reciprocal flow rate derivative, D/Mscf
s	Skin factor
t	Time, hr
$t^*m(P)'$	Pseudopressure derivative, psi^2/cp
$t^*\Delta P'$	Pressure derivative, psi^2/cp
T	Absolute Temperature, °R
u	Laplace space variable
x_e	effective reservoir width, ft
x_f	Hydraulic half-fracture length, ft
y^*	half-length of Stimulated Reservoir volume element, ft

Greeks

ϕ	Porosity, fraction
μ	Viscosity, cp

Suffices

g	Gas
i	Initial
D	Dimensionless
DA	Dimensionless based on drainage area
PSS	Pseudosteady state
sc	Standard conditions
L	Linear flow
LPSSi	Intersection point between linear flow and pseudosteady state.

ACKNOWLEDGEMENTS

The authors gratefully thank the Most Holy Trinity and the Virgin Mary mother of God for all the blessing received during their lives.

REFERENCES

El-Banbi A. H. and Wattenbarger R.A. 1998. Analysis of Linear Flow in Gas Well Production. Paper SPE 39972 presented at the SPE Gas Technology Symposium, Calgary, Alberta, Canada.

Escobar F.H., Montenegro L.M. and Bernal K.M. 2014. Transient-Rate Analysis For Hydraulically-Fractured Gas Shale Wells Using The Concept Of Induced Permeability Field. 9(7): 1244-1254.

Fuentes-Cruz G., Gildin E. and Valko P. 2014. Analyzing Production Data from Hydraulically Fractured Wells: the Concept of Induced Permeability Field. SPE Formation Evaluation. pp. 1-13.

Ge J. and Ghassemi A. 2011. Permeability Enhancement in Shale Gas Reservoirs after Stimulation by Hydraulic Fracturing. Paper AR11-514 presented at the Rock Mechanics / Geomechanics Symposium, San Francisco, CA.

Montenegro-G. L.M. and Bernal-V., K.M. 2014. Análisis del Comportamiento del Recíproco del Caudal y su Derivada en Función de Tiempo Adimensional en Yacimientos no Convencionales de Hidrocarburos - Gas Shale. B.Sc. Thesis. Universidad Surcolombiana. Neiva (Huila-Colombia). June.

Palmer I.D., Moschovidis Z.A. and Cameron J.R. 2007. Modeling Shear Failure and Stimulation of the Barnett Shale after Hydraulic Fracturing. Paper SPE 106113 presented at the SPE Hydraulic Fracturing Technology Conference, College Station, Texas, U.S.A.

Tiab D. 1993. Analysis of Pressure and Pressure Derivative without Type-Curve Matching: 1- Skin and Wellbore Storage. Journal of Petroleum Science and Engineering. 12: 171-181.

Wattenbarger R.A., El-Banbi A.H., Villegas M.E. and Maggard J. B. 1998. Production Analysis of Linear Flow into Fractured Tight Gas Wells. Paper SPE 39931 presented at the SPE Rocky Mountain Regional/Low Permeability Reservoirs Symposium, Denver, Colorado.

APPENDIX-A. GOVERNING EQUATIONS FOR OIL FLOW

A.1. Linear flow regime

The dimensionless equation representing the linear flow is independent of the model and the variation of permeability, the behavior is given by:

$$\left[t_D * P_D{}'\right] = \frac{5.74}{\pi}\sqrt{t_D} \tag{A.1}$$

In a similar fashion as Equation (20) was found for gas case, the linear skin factor for oil flow is given by:

$$s_L = 0.03\left(\frac{kt_L}{\phi\mu_o c_t x_e^2}\right)\left[\frac{\Delta P_L}{(t*\Delta P')_L} + \frac{1}{2}\right] \tag{A.2}$$

Once the dimensionless terms given by Equations (4) and (12) are plugged into Equation (A.1), the lateral extent of the stimulated reservoir volume can be solved for:

$$x_e = \frac{4.1894\ q\ \ B_o}{n_{HF}h\left[t*\Delta P'\right]_L}\sqrt{\frac{t_L}{\phi\mu_o c_t k^\circ}} \tag{A.3}$$

From the above equation it is possible to find the value of permeability:

$$k^\circ = \frac{17.5511 t_L}{\phi\mu_o c_t x_e^2}\left(\frac{q\ \ B_o}{n_{HF}h\left[t*(\Delta P)'\right]_L}\right)^2 \tag{A.4}$$

A.2. Pseudosteady-State Period

After replacing Equations (4) and (12) in Equation (22) and solving the reservoir length,

$$x_e = \frac{\pi(0.0002637)(141.2)\ q\ \ B_o}{n_{hf}\phi h\mu_o c_t y}\frac{t_{PSS}}{\left[t*\Delta P'\right]_{PSS}} \tag{A.5}$$

A.3. Intersection Point

A slight modification of Equation (25) is given here:

$$k^\circ = \left[\frac{1282.254 y^2\left[\phi\mu_o c_t\right]}{t_{LPSS_i}}\right] \tag{A.6}$$